Annales
Geophysicae

Injection and acceleration of H^+ and He^{2+} at Earth's bow shock

M. Scholer[1], H. Kucharek[1], K.-H. Trattner[2]

[1] Max-Planck-Institut für extraterrestrische Physik, 85740 Garching, Germany
[2] Lockheed Martin Missiles and Space, Palo Alto, CA 94304, USA

Abstract. We have performed a number of one-dimensional hybrid simulations (particle ions, massless electron fluid) of quasi-parallel collisionless shocks in order to investigate the injection and subsequent acceleration of part of the solar wind ions at the Earth's bow shock. The shocks propagate into a medium containing magnetic fluctuations, which are initially superimposed on the background field, as well as generated or enhanced by the electromagnetic ion/ion beam instability between the solar wind and backstreaming ions. In order to study the mass (M) and charge (Q) dependence of the acceleration process He^{2+} is included self-consistently. The upstream differential intensity spectra of H^+ and He^{2+} can be well represented by exponentials in energy. The e-folding energy E_c is a function of time: E_c increases with time. Furthermore the e-folding energy (normalized to the shock ramming energy E_p) increases with increasing Alfvén Mach number of the shock and with increasing fluctuation level of the initially superimposed turbulence. When backstreaming ions leave the shock after their first encounter they exhibit already a spectrum which extends to more than ten times the shock ramming energy and which is ordered in energy per charge. From the injection spectrum it is concluded that leakage of heated downstream particles does not contribute to ion injection. Acceleration models that permit thermal particles to scatter like the non-thermal population do not describe the correct physics.

Key words. Interplanetary physics (planetary bow shocks) · Space plasma physics (charged particle motion and acceleration; numerical simulation studies)

1 Introduction

Energetic ions with energies from just above solar wind energies to about 200 keV per charge upstream of the

Earth's bow shock have been studied extensively in the past. The upstream events can be divided according to their origin into two classes: the so-called magnetospheric bursts and the bow-shock associated events. The bow-shock associated events consist again of two distinctly different components: the reflected ions and the diffuse component (Gosling *et al.*, 1978). While the reflected component can be reasonably well understood by reflection of part of the solar wind ions at the quasi-perpendicular bow shock, the diffuse ions are believed to be due to a first-order Fermi acceleration process of solar wind ions in the converging flow at the quasi-parallel bow shock.

One of the most characteristic features of upstream diffuse ions is their spectral shape. Ipavich *et al.* (1981a) have shown that the spectrum of diffuse protons is quite different from a power law and that it can in fact be very well described by an exponential in energy $j \propto \exp(E/E_c)$. Furthermore, it was shown by Ipavich *et al.* (1981a) that the e-folding energy E_c is independent of ion species if represented in energy per charge (E/Q) units. Ipavich *et al.* (1981b) found that composition ratios in diffuse events were constant as a function of energy per charge not only during the equilibrium intensity levels of the events, but also during their onset and decay phases. Standard first order Fermi acceleration theory predicts, however, a spectral slope given by a power law independent from the upstream solar wind conditions and depending only on the shock compression ratio. In a statistical study of 382 upstream events it was found by Trattner *et al.* (1994) that the e-folding energy of upstream H^+ and He^{2+} spectra correlates with the solar wind velocity component parallel to the magnetic field.

To explain the exponential spectra, a number of models has been proposed which include a loss mechanism of some kind for the diffuse ions. The independence of the e-folding energy on ion species requires specific energy/charge dependencies of the acceleration efficiency, diffusion coefficients (mean free paths), and/ or of the loss processes. We will briefly summarize the

---

Correspondence to: M. Scholer

various mechanisms which possibly result in exponential spectra with an energy per charge independent scaling. For a detailed discussion see the review by Terasawa (1995).

In the parallel shock limit acceleration is only due to shock convergence which results in a species independent relative energy increase each time a particle experiences the shock compression. In this standard Fermi model the effect of an upstream free-escape boundary has been invoked in order to obtain exponential energy spectra (Forman, 1981; Ellison, 1981). In order to obtain the same e-folding energy in terms of energy/charge it is necessary that the upstream parallel diffusion coefficient $D_{\parallel}$ for different species is equal at the same E/Q. In quasi-linear theory of pitch angle diffusion $D_{\parallel}$ is given by

$$D_{\parallel} \propto \left(\frac{M}{Q}\right)^{(1-\delta)/2} \left(\frac{E}{Q}\right)^{(3-\delta)/2} \tag{1}$$

where δ is the power law index of the magnetic turbulence ($P \propto k^{-\delta}$, where k is the wave number). Therefore only $\delta = 1$ results in a diffusion coefficient $D_{\parallel}$ independent of M/Q at the same E/Q. However, upstream magnetic field power spectra can very rarely be represented by a power law with $\delta = 1$; in the lower k range δ may even be negative. A second model, which satisfactorily predicts energy spectra as measured, is the self-consistent model of Lee (1982). This model is based on an earlier model by Eichler (1981) which utilizes the three dimensional diffusion-convection equation including perpendicular diffusion. In this model particle loss is due to diffusion perpendicular to the magnetic field to the flanks of the bow shock, where the shock is weak, or to unconnected field lines. The solution of Lee (1982) can well be approximated by an exponential in energy. The e-folding energy is independent of the ion species if represented in E/Q and is independent of the form of the power spectrum of the upstream waves. The last property is due to the assumption of quasi-linear theory. However, the necessary perpendicular diffusion coefficient $D_{\perp}$ needed in order to explain the observations is rather large: Wibberenz *et al.* (1985) estimated that $D_{\perp}/D_{\parallel}$ has to be of the order of 0.7. Such a large perpendicular diffusion coefficient should lead to a considerable smoothing of lateral density gradients (Terasawa, 1995) which does not seem to be observed.

Terasawa (1995) has pointed out that relative energy increase $\Delta E/E$ is only in the exactly parallel limit independent of mass per charge M/Q. Terasawa (1981) has suggested that if there exists a tangential magnetic field component at the shock, and if the scattering mean free path is large compared to the shock transition region, particles should get directly reflected at the shock front. Mirror reflection at the shock leads to an energy gain per reflection of $\Delta E/E \propto (4V_1\mu)/v_i$, where v_i is the velocity of the ions, μ is the average of the pitch angle, and V_1 is the upstream plasma speed (Terasawa, 1995). This can be written as:

$$\frac{\Delta E}{E} \propto \left(\frac{M}{Q}\right)^{1/2} \left(\frac{E}{Q}\right)^{-1/2}. \tag{2}$$

The larger energy increase of higher M/Q particles at the same E/Q is due the larger drift path of the heavier ions. If the power law index of the upstream waves is less than 1, $D_{\parallel}$ is larger for larger M/Q particles at the same E/Q. Terasawa (1981) has suggested that this leads to a larger (upstream) escape probability which may cancel the larger acceleration efficiency, and could also lead to a E/Q regulation of the upstream spectrum.

Recently, hybrid simulations of quasi-parallel shocks have been used to study the microphysics of the shock transition layer and the process of particle acceleration self-consistently (Quest, 1988; Scholer, 1990; Kucharek and Scholer, 1991; Giacalone *et al.*, 1992). It has been shown by these simulations that a fraction of the solar wind thermal distribution is accelerated at the shock front by a coherent process. Kucharek and Scholer (1991) argued that these ions gain energy mainly due to a gradient B drift at the shock front. However, since the simulations were performed in the normal incidence frame, the apparent motion of an ion along the shock front in the coplanarity plane is simply the result of the motion of the field line in that frame. As has been shown recently by Scholer *et al.* (1998) a thermal solar wind particle reaches the shock and performs a nonadiabatic motion in the shock ramp during which the main velocity component v_x is re-directed into a tangential component. The particle then gyrates in the de Hoffmann-Teller frame near the shock ramp and is subject to the electric field of the upstream and shock generated waves. Acceleration occurs by the tangential electric field when the tangential velocity and the tangential electric field are nearly in phase, as proposed by Lyu and Kan (1993). The ion is decelerated when the tangential velocity is out of phase with the tangential electric field. The backstreaming accelerated ions constitute a seed particle population for subsequent further shock acceleration. Giacalone *et al.* (1992) have demonstrated by initially superimposing magnetic fluctuations on the background field that a downstream distribution of energetic ions is produced with a power–law slope that agrees well with the diffusive shock acceleration theory. Giacalone *et al.* (1993) extended these hybrid simulations and deduced the scattering law for protons in the upstream region. They obtained a diffusion length d which scales with energy approximately as $d \propto E^{1/3}$. Since $D(E) = d(E)v/3$ the diffusion coefficient scales with energy approximately as $E^{0.8}$. This would correspond, according to quasi-linear theory, to a power-law exponent of the magnetic field fluctuation spectrum of $\delta = 1.4$ and results in a weak dependence of the diffusion coefficient on mass per charge, $D_{\parallel} \propto (M/Q)^{-0.2}$. Ellison *et al.* (1990) could actually reproduce upstream spectra by a Monte Carlo simulation where they introduced a free escape boundary and assumed a mean free path determined by quasi-linear theory with $\delta = 1 \pm 0.5$. However, Giacalone *et al.* (1993) superimposed initially fluctuations with a power

spectral slope of $\delta = 1.5$ and a total power of $0.75B_1^2$, where B_1 is the upstream magnetic field strength. It is not clear to what degree the imposed high fluctuation level determines the final mean free path.

It has first been shown in the hybrid simulations of Trattner and Scholer (1991) that a fraction of solar wind He^{2+} is also extracted out of the solar wind at the shock and is further accelerated. This is rather important for the origin of upstream diffuse ions: alpha particles are considerably underabundant in the field-aligned beams originating at the quasi-perpendicular bow shock and these beams have therefore been dismissed as seed particles for diffuse ions. In the work by Trattner and Scholer (1991, 1994) H$^+$ and He^{2+} spectra have not been directly compared, and the diffusion coefficients have not been evaluated at the same energy per charge.

It is the purpose of the present paper to evaluate upstream spectra diffuse ion obtained in hybrid simulations of quasi-parallel shocks over a wide range of parameters. We will first investigate the dependence of proton spectra on the initially imposed upstream fluctuation level and on the shock Mach number. We will then include He^{2+} self-consistently and will try to elucidate which of the above mentioned scenarios results in these simulations in the energy per charge ordering of the spectra.

2 Simulation model

The hybrid model used in this paper treats the ions as macro-particles and the electrons as a charge-neutralizing, massless fluid (Winske and Leroy, 1984). Such a model reproduces satisfactorily observed ion scale length features of collisionless shocks. The simulation allows for one direction (shock normal direction x) and full three-dimensional velocities. The shock is launched by the rigid piston method: a plasma flows initially to the right of the simulation box and is being continuously supplied at the left boundary $x = 0$. The plasma is specularly reflected off a rigid, conducting wall, located at the right edge $x = L$ of the simulation domain. The reflected and incoming flow couple and lead to a shock which propagates to the left in the simulation frame, i.e., the simulation frame is the downstream rest frame. The upstream distance thus continuously shrinks as the simulation progresses. In the cases studied here the results were obtained when the shock was still sufficiently far from the left hand boundary (at least one diffusion length of the highest energy ions considered). Since the shock is known to accelerate only 2–3% of the incoming thermal ions, statistical valid distributions at higher energies can only be obtained by using an enormous number of thermal ions, which is not feasible, or by splitting particles as they increase in energy. The latter method has also been used in the recent hybrid simulations by Quest (1991), Scholer *et al.* (1992) and Giacalone *et al.* (1992). When a particle crosses an energy threshold it is split into two new particles which subsequently contribute each only half to the fields and plasma bulk moments. At the time of the splitting, the

position of the mother particle in phase space is unchanged, while the daughter is randomly displaced in the same spatial cell and has the same velocity. In the following simulations we have chosen 18 energy levels which are evenly spaced on a logarithmic scale in the range 1.5-150E_p (E_p = ramming energy of the solar wind plasma) for the protons and in the range 1.5-150E_p/Q for He^{2+}. This allows us to follow the distribution function over ten orders of magnitude.

Giacalone *et al.* (1992, 1993) have superposed on the initial, ambient magnetic field a spectrum of Alfvénic fluctuations. The injection of these waves was maintained at the left hand boundary of the simulation system. The rationale for this was that otherwise it takes too long to generate a fully matured upstream wave field within the simulation time. There are additional reasons which support the introduction of such a wave field when modeling the quasi-parallel bow shock: the interplanetary medium is turbulent on all scales. Furthermore, field-aligned beams produced at the quasi-perpendicular bow shock can excite waves by an electromagnetic ion/ion beam instability. These waves will subsequently be convected into the quasi-parallel regime. Both types of waves can be accounted for by the initial superposition of a wave field. As done by Giacalone *et al.* (1992, 1993), we assume the waves to be an equal mixture of right- and left-hand, forward- and backward propagating, circularly polarized coherent waves traveling with Alfvén velocity. Note that in a one-dimensional simulation the k wave vectors are forced in the simulation direction x. Since the upstream magnetic field makes an angle Θ_{Bn} with x this procedure does not give a correct initiation of magnetosonic or Alfvénic modes with k vectors in the x direction, unless $\Theta_{Bn} = 0$. Furthermore, we have not introduced corresponding perturbations in the bulk plasma properties. Rather, the simulation adjusts itself self-consistently after the start of the simulation and subsequently over a small region near the left edge of the injection boundary. The wave amplitudes are calculated by assuming a power spectrum in wave number, with a spectral index $\delta = 1.5$, i.e., $P(k) \propto k^{-1.5}$. There are 25 wave modes with wavelengths ranging from 5 to 400 ion inertial lengths. The total integrated spectral power is ϵB_1^2, where we have varied ϵ between 0.2 and 0.6.

In the simulations time is expressed in units of the inverse proton gyrofrequency $\Omega_{cp} = eB_1/(m_p c)$, where c is the speed of light, e is the magnitude of the electron charge and m_p is the proton mass. Distances are expressed in terms of the ion inertial length $\lambda = c/\omega_{pi}$, where ω_{pi} is the ion plasma frequency. The unit velocity is the upstream Alfvén velocity v_A; the unit density is then the upstream density n_1 and the unit magnetic field is the upstream magnetic field B_1. We used a grid size of $\Delta x = 0.5c/\omega_{pi}$ and the time step is $\Omega_{cp}\Delta t = 0.025$. In all runs the upstream plasma beta (ratio of plasma pressure to magnetic field pressure) for protons and electrons is held fixed at $\beta_i = \beta_e = 1.0$, and the angle Θ_{Bn} is assumed to be 5°. Two different box sizes are used: $L = 2000c/\omega_{pi}$ for the runs with H$^+$ only and $L = 1600c/\omega_{pi}$ for the run where He^{2+} is included self-consistently. In the latter run

we have assumed a He^{2+} to H$^+$ density ratio of $n_{He}/n_p = 0.05$ and a He^{2+} temperature of $T_{He} = 4T_p$, where T_p is the proton temperature. For comparison, one run with protons only was done in a very large simulation system of $L = 4000c/\omega_{pi}$.

3 Simulation results

In Fig. 1 we display spectra taken downstream of a $M_A = 4.1$ shock with different superimposed total integrated spectral power ϵ. The spectra represent spectral averages over $100c/\omega_{pi}$ downstream of the shock and are taken at the end of each simulation $T = 600\Omega_{cp}^{-1}$. At this time the shock is still $\sim 1340c/\omega_{pi}$ away from the upstream free-escape boundary. Plotted here and in the following figures is the differential intensity d$N(\tilde{v})$/d$\tilde{v}$, where $\tilde{v}$ is the velocity measured in a frame that is co-moving with the shock in units of the upstream plasma velocity v_{sw}, versus ramming energy $E_p = (m/2)v_{sw}^2$. The particle velocity v (in units of Alfvén velocity) divided by the Mach number results in the velocity $\tilde{v} = v/M_A$ in units of the ram (solar wind) velocity. The particles were sorted into logarithmically spaced bins of velocity $\tilde{v}$. The number of particles in each bin divided by $\tilde{v}$ results according to dN/d$\tilde{v}$ = $(1/\tilde{v})$ dN/d$(\log \tilde{v})$ in d$N(\tilde{v})$/d$\tilde{v}$. The unit of differential intensity is arbitrary but the same for all cases. The spectra are plotted in a logarithmic versus linear representation. Assuming a solar wind velocity of ~ 440 km/s the unit energy corresponds to ~ 1 keV. Note that the ram energy is determined by the solar wind speed and does not depend on Alfvén speed (i.e., is not given by the shock Mach

number). In all three cases the shock Alfvén Mach number is the same, $M_A = 4.1$. All Mach numbers given are in the shock frame of reference. Since the shock velocity and plasma properties continually change during the simulation, the Mach number is also time dependent and the value given is an average over the entire run. As can be seen from Fig. 1 the spectrum for $\epsilon = 0$ is close to an exponential in energy in the lower energy range and drops sharply off above some energy. The e-folding energy E_c in the lower energy range as well as the higher energy cut-off increases with increasing ϵ. At $\epsilon = 0.6$ the spectrum is an exponential up to the highest energy plotted. The important result to note is that the spectral e-folding energy depends strongly on ϵ, i.e., on the pre-existing magnetic field fluctuation level. In Fig. 2 we display the same spectra in a log–log representation. The spectra are offset by a factor 10 and we have indicated the energy scale only for the $\epsilon = 0$ spectrum. The spectra shown here can immediately be compared with those presented by Giacalone *et al.* (1993) and Ellison *et al.* (1993). They exhibit the pronounced flattening in the intermediate energy range and a steep drop-off to higher energies, as expected for an exponential. Since we are concerned in this paper with the measured exponential spectra in the 10–100 keV range, we will display in the following spectra only in the log versus linear version.

The backstreaming ions excite magnetosonic waves by an electromagnetic ion/ion beam instability. We have evaluated the spectral power in a region of $126c/\omega_{pi}$ upstream of the shock ramp. Figure 3 shows the total power in all three magnetic field components as a function of the absolute value of the wave vector k, where k is in units of inverse ion inertial length. In order to improve the power spectral presentation 20 spectral realizations obtained at different times during each run have been averaged. Shown are the power spectra for the cases $\epsilon = 0, 0.2$, and 0.6. The power spectra of the three cases are offset in k by one decade. In the case $\epsilon = 0$, i.e., without initially imposed upstream turbulence, the power spectrum peaks at $c/\omega_{pi}k \sim 0.2$. The
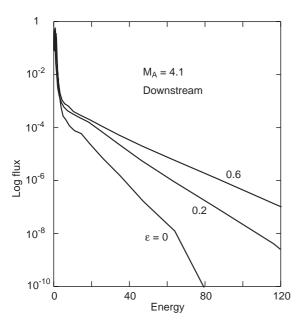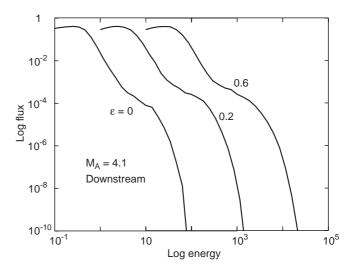

Fig. 1. Flux distributions for protons downstream of a $M_A = 4.1$ shock at $\Omega_{cp}t = 600$ in a log versus linear representation. Energy is measured relative to the shock frame of reference in units of the plasma ramming energy E_p. Different levels of initially superimposed fluctuations have been used ($\epsilon = 0, 0.2$ and 0.6)

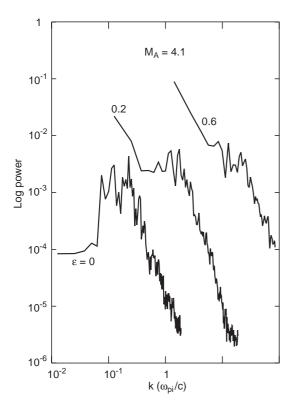**Fig. 2.** Same as Fig. 1 in a log–log representation

Fig. 3. Power spectra of the magnetic field fluctuations upstream of a $M_A = 4.1$ shock at $\Omega_{cp}t = 600$ for different upstream imposed turbulence levels ($\epsilon = 0, 0.2$, and 0.6). The spectra are offset by a factor 10

Fig. 4. Temporal development of the flux distribution at $\Omega_{cp}t = 600$ upstream of a $M_A = 5.4$ shock with $\epsilon = 0.2$

power spectral exponent is clearly positive for $c/\omega_{pi}k < 0.2$. With increasing superimposed upstream turbulence the peak disappears and at $\epsilon = 0.6$ the upstream power spectrum is largely determined by the superimposed wave field. Above $\epsilon = 0.6$ the power spectral slope is, on average, negative. Giacalone *et al.* (1992) used in their simulations $\epsilon = 0.75$ with $\delta = 1.5$. The finding that the diffusion coefficient scales as $D \propto E^{0.8}$ reflects most likely the power spectrum of the initially superimposed waves: these waves largely determine the final upstream fluctuation level. A spectral slope of $\delta = 1.5$ results according to quasi-linear theory in $D \propto E^{0.75}$. The result of Giacalone *et al.* (1992) should therefore be taken as a confirmation of quasi-linear theory and less as a determination of the energy dependence of the diffusion coefficient upstream of quasi-parallel shocks in the absence of background turbulence.

Power spectra of ULF waves upstream of the Earth's bow shock usually exhibit a hump at $\sim 0.02 - 0.03$ Hz (e.g., Le and Russell, 1992). We have therefore used in all subsequent runs a fluctuation level given by $\epsilon = 0.2$, which results in power spectra close to spectra which are actually observed. Figure 4 shows the temporal development of the downstream intensity spectrum for the $M_A = 5.4$ case. These and the following spectra shown are spectral averages over $100c/\omega_{pi}$ upstream of the shock. Note that under typical solar wind conditions at 1 AU $1\Omega_{cp}^{-1}$ corresponds to ~ 1 s and E_p corresponds to
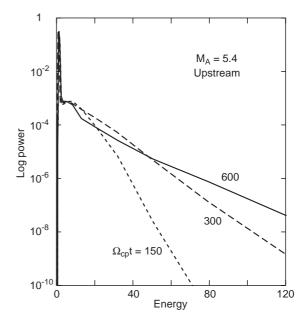
~ 1 keV. It is evident that the intensity up to $\sim 30E_p$ appears within $\Omega_{cp}t = 150$ and is rather constant with time, whereas at an energy of $\sim 150E_p$ the intensity continuously rises. This leads to the so-called inverse energy dispersion observed during many upstream particle events. In the lower energy range the events usually exhibit a flat top profile (Ipavich *et al.*, 1981b) which is consistent with the simulation. An increase in the far upstream magnetic field power level ϵ considerably speeds up the flattening of the spectrum. When we use $\epsilon = 0.6$ the intensity reaches within $\sim 150\Omega_{cp}^{-1}$ more or less a steady state up to $\sim 60E_p$. The field-aligned beams near the quasi-perpendicular shock can excite electromagnetic waves, so that when these waves are convected into the quasi-parallel regime the power at the edges of upstream events may actually be increased. In the case of a non-radial interplanetary magnetic field (IMF) this may considerable reduce the inverse energy dispersion effect.

The assumption of free particle escape as a boundary condition is an unavoidable artifact in the hybrid simulations of collisionless shocks. But the necessity of a free escape boundary in hybrid and Monte Carlo simulations should not be confused with the introduction of a free escape boundary in any steady state theory: as pointed out in the introduction, the free escape boundary has also been employed in order to obtain exponential spectra in a steady state Fermi acceleration model. In order to prove that the spectrum is largely independent of the position of this artificial boundary in the simulations we have repeated the $M_A = 5.4$ shock run in a numerical box of twice the original size. Figure 5 compares the spectrum obtained by a run in a box with a size of $L = 2000c/\omega_{pi}$ with the spectrum obtained in a box with size $L = 4000c/\omega_{pi}$. At the end of the run the upstream region extends
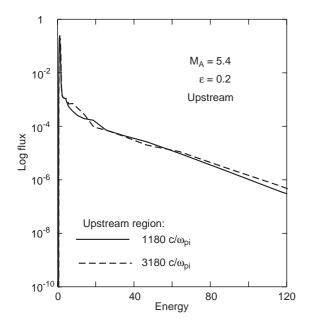
Fig. 5. The flux distribution upstream of a $M_A = 5.4$ shock with $\epsilon = 0.2$ for two different simulation box sizes, $L = 2000c/\omega_{pi}$ and $L = 4000c/\omega_{pi}$

Fig. 6. Dependence of the upstream flux distribution at $\Omega_{cp}t = 600$ on Alfvén Mach number M_A. Shown are results from 3 cases: $M_A = 4.1, 5.4$, and 7.3

$L_u = \sim 1180c/\omega_{pi}$ and $L_u = \sim 3180c/\omega_{pi}$, respectively, from the shock to the left hand free escape boundary. In the latter case this corresponds in real units to more than $50\ R_E$ upstream of the Earth's bow shock. Both spectra are obtained by averaging over $100c/\omega_{pi}$ upstream of the shock ramp. As can be seen from Fig. 5, differences are indeed minor. Thus, the actual location of the left hand boundary has no influence yet on the spectra close to the shock and in the region downstream (not shown here). This is of course due to the chosen values of Mach number and distance L_{esc} to the free escape boundary. Giacalone *et al.* (1997) have estimated the time τ_a as a function of Mach number and L_{esc} so that for times larger than τ_a the spectra will be determined by the free escape boundary, while for times shorter than τ_a the spectrum is still evolving. Our value of maximum run time is still smaller than τ_a, so that the result in Fig. 5 is consistent with the Giacalone *et al.* (1997) estimates. There exists no free escape boundary in nature; if the simulated spectra would have been determined by the free escape boundary, the simulation system has to be increased. In the present simulations the distance L_{esc} between shock and free escape boundary continuously decreases during the simulation run. We note in passing that a different approach was taken by Ellison *et al.* (1993). In their simulations the free escape boundary tracked the shock, so that L_{esc} stayed constant with time.

Figure 6 shows the dependence of the upstream intensity spectrum on shock Alfvén Mach number. Here, the results for three cases, $M_A = 4.1, 5.4$ and 7.3 are compared. The e-folding spectral energy E_c increases strongly with increasing Mach number: at $M_A = 4.1$ we find $E_c = 8.6E_p$, at $M_A = 5.4$ we obtain $E_c = 16.6E_p$, and at $M_A = 7.3$ the spectrum can be fit with an exponential with $E_c = 22.5E_p$. Note that the energy is expressed in
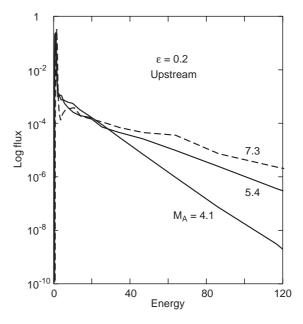
units of the shock ram energy and is independent of the Alfvén velocity. The result shown in Fig. 6 predicts flatter upstream diffuse ion spectra for a solar wind with the same Alfvén speed but higher solar wind velocity since the Mach number increases. The e-folding energies obtained here are well within the observed range (Trattner *et al.* 1994). The flatter spectrum in the high Mach number case results in a higher energy density of upstream ions. This, in turn, should lead to an increase in the upstream power spectrum. Figure 7 shows the upstream magnetic field power for 3 Mach number cases. The spectra are again shifted in k by one decade against each other. As expected the power indeed increases with increasing Mach number, and the spectral hump moves with increasing Mach number to smaller k.

We will now discuss results of a simulation where He^{2+} is included self-consistently. Figure 8 shows the H$^+$ and He^{2+} spectra at the end ($\Omega_{cp}t = 450$) of a $M_A = 5.4$ run. The spectra are again averaged over a region of $100c/\omega_{pi}$ upstream and downstream of the shock ramp, respectively. The spectra are represented as differential flux versus energy per charge, $(E/E_p)/Q$, in a logarithmic versus linear representation. Both spectra can be very well represented over the entire energy/charge range by an exponential in energy/charge. Moreover, since both lines are parallel to each other, the e-folding energy is identical for H$^+$ and He^{2+} when expressed in terms of energy per charge. This simulation result is in accordance with measurements of upstream spectra, as outlined in the introduction. The He^{2+} to H$^+$ ratio of the diffuse ion fluxes is enhanced by about a factor 5 relative to same ratio in the solar wind. Enhancements of He^{2+} relative to H$^+$ in diffuse ion events have been reported by Ipavich *et al.* (1981b) and more recently by Fuselier (1994).
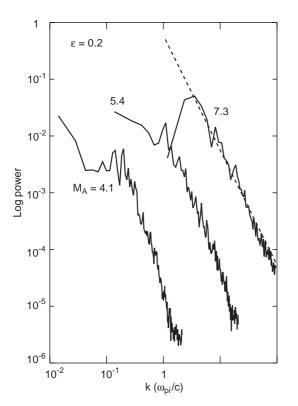
Fig. 7. Power spectra of the magnetic field upstream of a $M_A = 4.1, 5.4$, and 7.3 shock

In Fig. 9 we have plotted the energy/charge of every fifth upstream ion versus the drift length ζ in the z direction. The length ζ is calculated as $\zeta = \int h \, dz = \int h v_z \, dt$, where $h = 1$ if the particle is within one gyroradius of the shock ramp, and $h = 0$ otherwise. The drift is calculated in the de Hoffmann-Teller frame, i.e., the velocity v_z has been transformed from the normal incidence frame into the de Hoffmann-Teller frame. The upper part shows the result for the protons and the lower part shows the result for the He^{2+}. As can be seen, the average drift is about zero, i.e., the particles stay essentially in the same flux tube. The spread in ζ increases with increasing energy/charge mainly since the gyroradius increases. Figure 10 shows the energy/charge of every fifth upstream ion versus the total time τ the particle has spent near the shock ramp. The time τ is calculated as $\tau = \int h \, dt$. Both species spent about the same time near the shock ramp and the energy/charge is correlated with that time.

In order to determine the scattering law we employ steady state diffusion theory which predicts that the density of energetic ions falls off exponentially from the shock ramp into the upstream region with an e-folding distance given by $D_\parallel / V_1$, where V_1 is the upstream plasma flow speed relative to the shock frame. In Fig. 11 we display the logarithm of the H$^+$ and He^{2+} partial densities as a function of position within the energy per charge bands indicated in the respective panel. The arrows in the upper and lower panels indicate the position of the shock ramp. In the $16 \le (E/E_p)/Q \le 25$ energy range the H$^+$ and He^{2+} partial densities track each other, i.e., the ratio of He^{2+} to H$^+$ in this energy
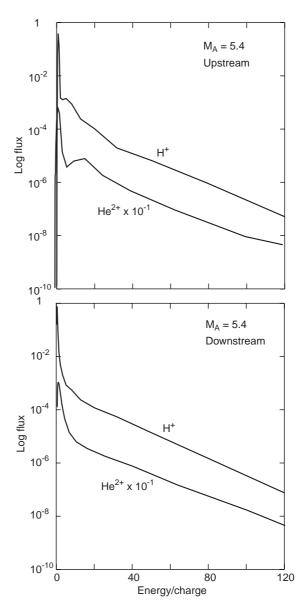

Fig. 8. The flux distributions of protons and alpha particles upstream (**a**) and downstream (**b**) of the $M_A = 5.4$ shock at $\Omega_{cp}t = 450$

per charge range is about constant. We thus conclude that in this $(E/E_p)/Q$ band the diffusion coefficient is approximately independent of mass per charge, M/Q. In the $9 \le (E/E_p)/Q \le 16$ band (upper panel) the protons drop off faster with distance upstream than the alpha particles. Consequently, the He^{2+} to H$^+$ ratio increases with upstream distance, indicating that the diffusion coefficient in this energy per charge range decreases with increasing M/Q. The opposite is true for the $49 \le (E/E_p)/Q \le 64$ energy per charge band: here, the He^{2+} to H$^+$ ratio increases with distance upstream, i.e., the diffusion coefficient increases with increasing M/Q. Such a behavior of $D_\parallel$ is consistent with quasi-linear theory: towards lower $|k|$ the magnetic field power spectrum becomes flatter or turns over, which results, according to Eq. (1), in an increase of $D_\parallel$ with M/Q for those particles which resonate with large wavelength
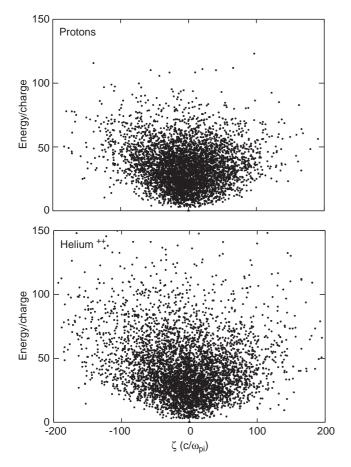
Fig. 9. Energy per charge in units of the shock ram velocity E_p of upstream ions versus drift length ζ in the de Hoffmann-Teller frame. **a** protons; **b** alpha particles

Fig. 10. Energy per charge in units of the shock ram velocity E_p of upstream ions versus time τ spent at shock. **a** protons; **b** alpha particles

waves, i.e., high energy per charge ions. Lower energy particles resonate with small wavelength (large k) waves. Here, the power spectral exponent $\delta > 1$, which results in a smaller diffusion coefficient for the M/Q species. It has to be kept in mind that this approach assumes a steady state, whereas according to the simulation the spectra still develop in time.

We will demonstrate now that the diffuse ions are already injected at the shock with an energy spectrum extending to several tens of the ram energy and that already the injection spectra of protons and He^{2+} track each other in energy per charge. During the run the velocity of a backstreaming ion is registered when the ion crosses for the first time a boundary immediately ($10c/\omega_{pi}$) upstream of the shock ramp in the upstream direction. When at the end of the run a backstreaming ion is found more than $30c/\omega_{pi}$ upstream it is counted as a diffuse ion. Figure 12 (upper panel) shows the number of backstreaming ions versus velocity and energy per charge $(E/E_p)/Q$ (lower panel) when they crossed for the first time the boundary immediately upstream of the shock ramp. This distribution can be considered as the injection spectrum. It can be seen from the upper panel that a large contribution to the proton and He^{2+} ion injection spectra consists of ions, which in the shock frame have about shock ram
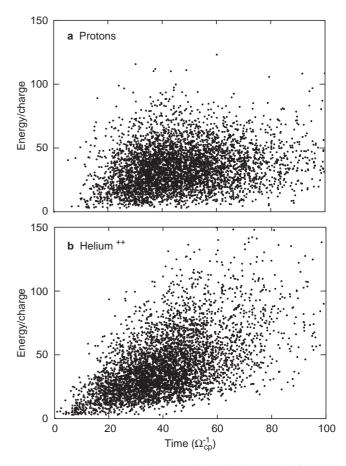
velocity, i.e., which are specularly reflected at the shock. The injection spectrum of H$^+$ and He^{2+} extends to several tens of the shock ram energy and is almost identical for both species when evaluated at equal energy per charge (lower panel).

As can be seen from Fig. 12 (top panel) the number of injected ions drops drastically to zero for velocities smaller than the shock ram velocity v_r. The distributions in Fig. 12 are plotted in the shock frame. As shown schematically in Fig. 13 in the shock rest frame the hot downstream distribution is moving with a bulk velocity U_2. The tail of the distribution with upstream directed velocities ($v_x < 0$) are, in principle, able to leak upstream. This population has the highest intensity at $v_x \rightarrow 0$ and the intensity decreases with $|-v_x|$. Since the intensity of the injection spectrum does not increase, but decreases with $v/v_r \rightarrow 0$, we conclude that leakage does not represent a significant contribution to ion injection at quasi-parallel shocks. Acceleration models which relay on heated downstream ions injected into a first order Fermi process under the assumption of an ad hoc scattering law may result in observed spectra and abundances, but do not describe the appropriate physics.
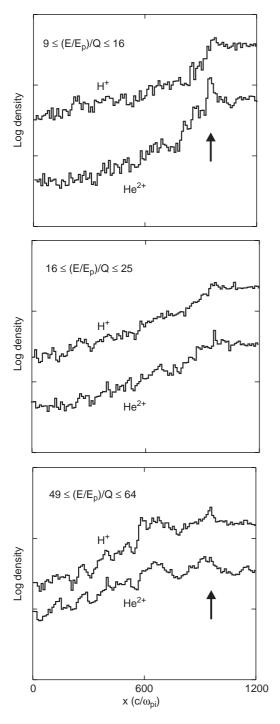
Fig. 11. Logarithm of the partial density of protons and alpha particles in three energy per charge bands versus distance. The position of the shock is indicated by an *arrow*
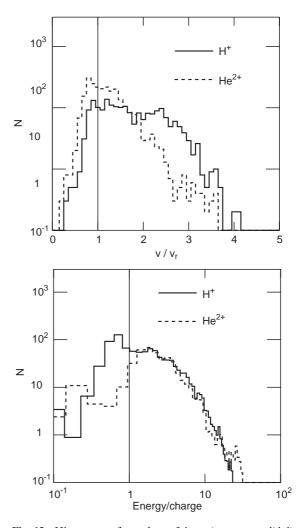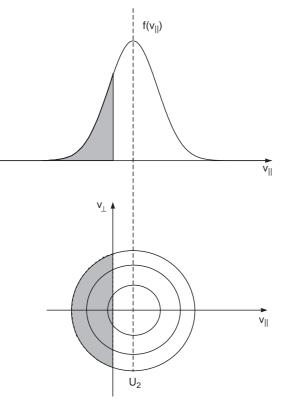

Fig. 12. Histogram of number of ions (protons: *solid line*; alpha particles: *dashed line*) versus velocity in units of shock velocity (*upper panel*) and versus energy per charge in units of shock ramming energy (*lower panel*), when the ions cross for the first time a boundary located at $10c/\omega_{pi}$ in front of the shock in th upstream direction

4 Discussion

We have performed a large number of quasi-parallel shock simulations over a wide range of Mach numbers and assuming different fluctuation levels initially superimposed on the background magnetic field. In a number of these simulations He^{2+} has been self-consistently included. The particle splitting technique allows us to follow the particle intensity over ten orders of magnitude. With respect to the ongoing discussion of bow shock acceleration versus magnetospheric leakage we would like to stress that we make no assumptions concerning the occurrence of a Fermi type process; we simply solve self-consistently the equations of motion for the particles and the appropriate equations for the fields. As has already been demonstrated in earlier work by Scholer (1990), Kucharek and Scholer (1991), Giacalone *et al.* (1992) and Giacalone *et al.* (1993) these simulations result in upstream diffuse ions which extend in energy up to more than 100 times the shock ram energy. The specific results of the present investigation can be summarized as follows:

1. The differential spectra of H$^+$ and He^{2+} at a quasi-parallel shock can be well represented by exponentials in energy. The e-folding energy E_c is a function of time: E_c increases with time. The e-folding energy normalized to the shock ramming energy E_p increases with increasing Alfvén Mach number and with increasing fluctuation level of the initially superimposed turbulence.

Fig. 13. Schematic showing the downstream reduced distribution function $f(v_{\parallel})$ in the shock frame centered around the downstream bulk speed U_2. The lower part shows iso-intensity contours of f. Ions in the *shaded part* have an upstream directed velocity and contribute to leakage

2. The upstream magnetic field power spectra exhibit a hump around $c/\omega_{pi}k = 0.1$. The hump disappears below the background power if the power in the initially superimposed fluctuations is higher than $\sim 0.6B_1^2$, where B_1 is the upstream magnetic field strength. The power increases with increasing Mach number and the position of the hump shifts to smaller k.

3. The upstream spatial diffusion coefficient at the same energy per charge decreases in the low E/Q range with increasing mass per charge. At the high E/Q end the diffusion coefficient increases with increasing M/Q.

4. H$^+$ and He^{2+} gyrate near the shock ramp and are subject to the electric field of the upstream and shock generated waves. The injection spectrum consists of specularly reflected ions and a higher energy population. The injection spectrum of the higher energy population is already ordered in energy per charge $(E/E_p)/Q$.

The fact that energy spectra can be well represented by exponentials reflects the importance of time dependence in the acceleration process. The increase of E_c with time and Mach number can be explained by diffusive shock acceleration theory. For the time-dependent case the power law cut off momentum p_c is governed by (Drury, 1983; Jokipii, 1987)

$$\frac{1}{p_c}\frac{dp_c}{dt} \propto \frac{U_1}{\kappa_1} \qquad (3)$$

with U_1 as the upstream flow speed and κ_1 as the upstream diffusion coefficient. Thus p_c increases with time and is larger at the same time for larger Mach number shocks. The ion/ion beam instability between the backstreaming ions and the solar wind is considerably enhanced by a small level of initially superimposed fluctuations. At $\Omega_{cp}t = 600$ (corresponding to ~ 10 min real time) the intensity at $E/E_p = 30$ (corresponding to ~ 30 keV) is two orders of magnitude smaller when no fluctuations are initially present as compared to the case when the shock runs into a solar wind with far upstream magnetic field fluctuations corresponding to a total power of $0.2B_1^2$. We suggest that the absence of diffuse ions under conditions of long interplanetary magnetic field–bow shock connection times can be explained by an extremely quiet background field. Diffuse ion fluxes may be below instrument's thresholds and can be observed with sufficient counting statistics only below a few keV.

Results 2 and 4 are consistent with quasi-linear theory. To a first approximation the dispersion relation for upstream waves can be written as $\omega = kv_A$. Excitation of hydromagnetic waves by backstreaming ions with velocity v_b is expected when the cyclotron resonance condition $\omega - k_r v_b = -\Omega_{cp}$ is fulfilled. Let us assume that close to the shock the majority of backstreaming ions have in the solar wind frame about twice the solar wind speed, corresponding to specular reflection, and that the solar wind has an average Alfvén Mach number of 5, we obtain in dimensionless units $k_r \approx 0.1$. This is where the spectral hump is indeed found. Higher Mach number shocks result in flatter spectra; the presence of higher velocity particles shifts the position of cyclotron resonance to smaller values of k. The dependence of the upstream diffusion coefficient on mass per charge is as predicted by quasi-linear theory: high energy per charge ions resonate with waves whose k vectors are smaller than k_r. Here the power spectral slope is zero or even positive. At high energies the upstream diffusion coefficient and thus the characteristic upstream distance of the partial density of He^{2+} should therefore be larger than that of protons at the same energy per charge.

The above consideration is based on the simplifying assumption that specularly reflected ions mainly excite the upstream waves. However, the higher energy diffuse ions extend further upstream than lower energy diffuse ions. At the foreshock boundary, i.e., far upstream, these ions will first excite waves with larger wavelengths, which are then convected toward the shock. Closer to the shock lower energy particles will excite waves with smaller wavelength. The increase of the magnetic field power with increasing Mach number cannot be predicted by quasi-linear theory. There is almost an order of magnitude increase in the power between $\sim M_A = 4$ and $\sim M_A = 7$ shocks. When the large amplitude fluctuations at high Mach number are convected into the shock they lead to a large wave electric field which is

experienced by part of the particle population. This, in turn, leads to a first step acceleration to higher energies, i.e., the upstream spectrum is flatter at higher Mach numbers. The production of flat spectra and large fluctuation levels is self-sustaining: the high energy content in the diffuse ions leads by the ion/ion beam instability to the large-amplitude pulsations; when these pulsations hit the shock they in turn lead to large temporal electric fields which some particles will experience.

The ordering of upstream spectra in terms of energy per charge in the simulations can neither be explained in terms of the mirror reflection nor in terms of the standard steady state Fermi model. The Fermi model assumes a species independent relative energy increase each time a particle experiences the shock compression. The effect of an upstream free escape boundary in combination with an M/Q independent diffusion coefficient at the same E/Q has been invoked in order to obtain exponential energy spectra with the same E_c/Q for H^+ and He^{2+}. Both seem not to be the case: the diffusion coefficient depends, although only slightly, on M/Q, with the dependence varying over the energy per charge range considered. The ions, which become diffuse ions, gyrate during their first encounter with the shock near the shock ramp and are subject to the electric field of the upstream and shock generated waves. As proposed by Lyu and Kan (1992) acceleration occurs when the tangential velocity of the ion and the tangential electric field are nearly in phase. The energy gain in an electric field depends on the particle's charge. Since both species are trapped near the shock for the same time, He^{2+} gains twice the energy than protons, which is expected to result in an ordering of upstream spectra in terms of energy per charge. This does not explain why a certain part of the upstream ions stay for an extended time period near the shock nor why protons and alpha particles spend on average the same time near the shock.

The simulations presented here have shown that at least up to $\Omega_{cp}t = 600$ the behavior of the spectrum near the shock and downstream evolves with time. From the comparison of two runs with vastly different simulation system sizes it is concluded that the spectral shape is not due to the existence of a free escape boundary, but due to time dependence. The free escape boundary has been invoked in order to deal with a time dependent acceleration process at the bow shock in terms of steady state first order Fermi theory. If using a steady state theory with a free escape boundary as a proxy for time dependent acceleration the position of the free escape boundary should depend on time, as well as on energy and M/Q of the species considered. In order to explain the energy per charge ordering of spectra within the framework of steady state Fermi theory with a species independent location of the free escape boundary, the diffusion coefficient has to be independent of M/Q at the same E/Q. The present self-consistent simulations suggest that the ordering of the shock spectra in terms of energy/charge is not determined by the M/Q dependence of the diffusion coefficient in the upstream region, but by the injection and acceleration processes at the shock

itself. Since the ions are accelerated by the wave electric field this naturally results in a E/Q ordering. The present simulations do not take into account diffusive transport normal to the magnetic field and lateral free escape along disconnected field lines. As outlined in the introduction, a model invoking cross field diffusion is also capable of explaining the energy per charge ordering of upstream spectra. However, as shown here, there is no immediate need for such a model and the mechanism present in the self-consistent one-dimensional simulations results in the observed spectral shape and energy per charge ordering.

Some of the results presented here are different from the results in the work of Giacalone *et al.* (1992) and Giacalone *et al.* (1993); the reason is that these authors used rather high values of the initially superimposed power in the magnetic field fluctuations. This is not meant as a critique but rather as a clarification: Giacalone *et al.* (1992) were interested in rapidly reaching high energies and in obtaining power law spectra as predicted by steady state Fermi theory. They achieved this by assuming a high fluctuation level and consequently small mean free paths. However, we feel that this is not appropriate for bow shock investigations.

The simulations allow a number of predictions for observations at the Earth's bow shock. The time dependence of upstream spectra translates in a dependence of the spectra on time of connection between the IMF and the bow shock. For average magnetic field conditions harder spectra are predicted the more one moves from noon to earlier local time. The e-folding energy of upstream spectra should strongly depend on Mach number. It also depends on solar wind velocity at the same Mach number: the scaling of the upstream spectra is given in shock ram energy. At the same Mach number a higher solar wind speed results (in real units) in a larger e-folding energy. It should be remembered that the simulations are performed in the normal incidence frame. Thus, e-folding energies will also depend on the IMF cone angle. The prediction of larger upstream e-folding distances for He^{2+} than for H^+ at large E/Q values is consistent with the statistical findings by Trattner *et al.* (1994; cf. their Figs. 8 and 10). Many events do not exhibit a clear inverse velocity dispersion. It is suggested that these events are due to a slow change from quasi-perpendicular to quasi-parallel. The field-aligned beams from the quasi-perpendicular bow shock excite electromagnetic ion/ion beam instabilities and the resulting turbulence is convected into the quasi-parallel to quasi-perpendicular shock transition region. The high fluctuation level in this region may lead to harder spectra. A spacecraft moving slowly into the quasi-parallel regime due to a change of the magnetic field cone angle may then see a harder spectrum earlier and could even observe a spectral softening as it moves into the quasi-parallel regime proper.

There are a number of open questions which have to be addressed in future work. In particular, the question why a certain part of the upstream ion distribution stays near the shock and is not transmitted downstream has to be answered by analyzing individual orbits in detail.

Also of importance is the question of acceleration efficiency, i.e., what regulates the number of ions which are accelerated in the first step acceleration process. Preliminary results have shown that this efficiency is controlled by the upstream waves: eliminating upstream waves (by attributing zero weight to backstreaming ions) leads to a reflection of more than 40% of the incoming solar wind population. Thus the processes of injection efficiency and upstream wave generation are self-regulating.

References

Drury, L. O'C., An introduction to the theory of diffusive shock acceleration of energetic particles in tenuous plasmas, *Rep. Progr. Phys.*, **46**, 973, 1983.

Eichler, D., Energetic particle spectra in finite shocks: the Earth's bow shock, *Astrophys. J.*, **244**, 711, 1981.

Ellison, D. C., Monte Carlo simulation of charged particles upstream of the Earth's bow shock, *Geophys. Res. Lett.*, **8**, 991, 1981.

Ellison, D. C., E. Möbius, and G. Paschmann, Particle injection and acceleration at the Earth's bow shock: comparison of upstream and downstream events, *Astrophys. J.*, **352**, 376, 1990.

Ellison, D. C., J. Giacalone, D. Burgess, and S. J. Schwartz, Simulations of particle acceleration in parallel shocks: direct comparison between Monte Carlo and one-dimensional hybrid codes, *J. Geophys. Res.*, **98**, 21,085, 1993.

Forman, M. A., First order Fermi acceleration of the diffuse ion population near the Earth's bow shock, *Proc. Int. Conf. Cosmic Rays*, 17th, 467, 1981.

Fuselier, S. A., A comparison of energetic ions in the plasma depletion layer and the quasi-parallel magnetosheath, *J. Geophys. Res.*, **99**, 5855, 1994.

Giacalone, J., D. Burgess, S. J. Schwartz, and D. C. Ellison, Hybrid simulations of protons strongly accelerated by a parallel collisionless shock, *Geophys. Res. Lett.*, **19**, 433, 1992.

Giacalone, J., D. Burgess, S. J. Schwartz, and D. C. Ellison, Ion injection and acceleration at parallel shocks: comparison of self-consistent plasma simulations with existing theories, *Astrophys. J.*, **402**, 550, 1993.

Giacalone, J., D. Burgess, S. J. Schwartz, D. C. Ellison, and L. Bennett, Injection and acceleration of thermal protons at quasi-parallel shocks: a hybrid simulation parameter survey, *J. Geophys. Res.*, **102**, 19,789, 1997.

Gosling, J. T., J. R. Asbridge, J. Bame, G. Paschmann, and N. Sckopke, Observations of two distinct populations of bow shock ions in the upstream solar wind, *Geophys. Res. Lett.*, **5**, 957, 1978.

Ipavich, F. M., A. B. Galvin, G. Gloeckler, M. Scholer, and D. Hovestadt, A statistical survey of ions observed upstream of the Earth's bow shock: energy spectra, composition, and spatial variations, *J. Geophys. Res.*, **86**, 4337, 1981a.

Ipavich, F. M., M. Scholer, and G. Gloeckler, Temporal development of composition, spectra, and anisotropies during upstream particle events, *J. Geophys. Res.*, **86**, 11,153, 1981b.

Jokipii, J. R., Rate of energy gain and maximum energy in diffusive shock acceleration, *Astrophys. J.*, **3313**, 842, 1987.

Kucharek, H., and M. Scholer, Origin of diffuse superthermal ions at quasi-parallel supercritical collisionless shocks, *J. Geophys. Res.*, **96**, 21195, 1991.

Le, G., and C. T. Russell, A study of ULF wave foreshock morphology-II: Spatial variations of ULF waves, *Planet. Space Sci.*, **40**, 1215, 1992.

Lee, M. A., Coupled hydromagnetic wave excitation and ion acceleration upstream of the Earth's bow shock, *J. Geophys. Res.*, **87**, 5063, 1982.

Lyu, L. H., and J. R. Kan, Ion dynamics in high-Mach number quasi-parallel shocks *J. Geophys. Res.*, **98**, 18985, 1993.

Quest, K. B., Particle injection and cosmic ray acceleration at collisionless parallel shocks, in *Proceedings of 6th International Solar Wind Conference*, Techn. Note 306, p. 503, Natl. Cent. Atmos. Res., Boulder, Colo., 1988.

Quest, K. B., Acceleration of diffuse ions upstream from parallel shocks, in *Particle Acceleration in Cosmic Plasmas*, eds. G. P. Zank and T. K. Gaisser, AIP Conf.Proc. **264**, American Inst. of Physics, New York, p. 348, 1991.

Scholer, M., Diffuse ions at quasi-parallel shocks: simulations, *Geophys. Res. Lett.*, **17**, 1821, 1990.

Scholer, M., K. J. Trattner, and H. Kucharek, Ion injection and Fermi acceleration at Earth's bow shock: the 1984 September 12 event revisited, *Astrophys. J.*, **395**, 675, 1992.

Scholer, M., H. Kucharek, and K. J. Trattner, Injection and acceleration of energetic particles at collisionless shocks, *Adv. Space Res.*, **21**, 533, 1998.

Terasawa, T., Energy spectrum of ions accelerated through Fermi process at the terrestrial bow shock, *J. Geophys. Res.*, **86**, 7595, 1981.

Terasawa, T., Ion acceleration, *Advances Space Res.*, **15**, 53, 1995.

Trattner, K. J., and M. Scholer, Diffuse alpha particles upstream of simulated quasi-parallel supercritical shocks, *Geophys. Res. Lett.*, **18**, 1817, 1991.

Trattner, K. J., and M. Scholer, Diffuse minor ions upstream of simulated quasi-parallel shocks, *J. Geophys. Res.*, **99**, 6637, 1994.

Trattner, K. J., E. Möbius, M. Scholer, B. Klecker, M. Hilchenbach, and H. Lühr, Statistical analysis of diffuse ion events upstream of the Earth's bow shock, *J. Geophys. Res.*, **99**, 13,389, 1994.

Wibberenz, G., F. Zöllich, and H. M. Fischer, Dynamics of intense upstream ion events, *J. Geophys. Res.*, **90**, 283, 1985.

Winske, D., and M. M. Leroy, Hybrid simulation techniques applied to the Earth's bow shock, in *Computer Simulation of Space Plasmas*, edited by H. Matsumoto and T. Sato, p. 255, Kluwer Academic, Norwell, Mass., 1984.